NAVAL POSTGRADUATE SCHOOL
Monterey, California

THESIS

MULTI-SCALE ANALYSIS OF A 2/2-TWILL WOVEN FABRIC COMPOSITE

by

Kevin K. Roach

March 2002

Thesis Advisor: Young W. Kwon

Approved for public release; distribution is unlimited

THIS PAGE INTENTIONALLY LEFT BLANK

REPORT DOCUMENTATION PAGE			Form Approved OMB No. 0704-0188
Public reporting burden for this collection of information is estimated to average 1 hour per response, including the time for reviewing instruction, searching existing data sources, gathering and maintaining the data needed, and completing and reviewing the collection of information. Send comments regarding this burden estimate or any other aspect of this collection of information, including suggestions for reducing this burden, to Washington headquarters Services, Directorate for Information Operations and Reports, 1215 Jefferson Davis Highway, Suite 1204, Arlington, VA 22202-4302, and to the Office of Management and Budget, Paperwork Reduction Project (0704-0188) Washington DC 20503.			
1. AGENCY USE ONLY ***(Leave blank)***	**2. REPORT DATE** March 2002	**3. REPORT TYPE AND DATES COVERED** Master's Thesis	
4. TITLE AND SUBTITLE: Multi-Scale Analysis of a 2/2-Twill Woven Fabric Composite.			**5. FUNDING NUMBERS**
6. AUTHOR(S) **Kevin K. Roach**			
7. PERFORMING ORGANIZATION NAME(S) AND ADDRESS(ES) Naval Postgraduate School Monterey, CA 93943-5000			**8. PERFORMING ORGANIZATION REPORT NUMBER**
9. SPONSORING /MONITORING AGENCY NAME(S) AND ADDRESS(ES) N/A			**10. SPONSORING/MONITORING AGENCY REPORT NUMBER**
11. SUPPLEMENTARY NOTES The views expressed in this thesis are those of the author and do not reflect the official policy or position of the Department of Defense or the U.S. Government.			
12a. DISTRIBUTION / AVAILABILITY STATEMENT Approved for public release; distribution is unlimited			**12b. DISTRIBUTION CODE**

13. ABSTRACT ***(maximum 200 words)***

A micro-mechanical unit-cell model was developed for 2/2-twill woven fabric composites. A multi-scale bi-directional micro/macro-mechanical analysis technique was applied to the model in an effort to estimate effective material properties of 2/2-twill composites and decompose the effective stresses (strains) of the woven fabric composite into the stresses (strains) of the tows. When this unit-cell model is incorporated into the multi-scale analysis by combining with previously developed modules, the residual strength and stiffness of a laminated structure made of 2/2-twill woven fabric composites can be predicted along with damage progression in the structure. Damage is described at the basic material units of the composite structure, the fibers and matrix. The unit-cell model and the multi-scale analysis were validated by comparing their predicted results to available data in open literature and data obtained from a finite element models.

14. SUBJECT TERMS Multilevel Technique, Woven Fabric Composite, 2/2-twill Composite, Microanalysis, Macro analysis			**15. NUMBER OF PAGES** TOTAL #56
			16. PRICE CODE
17. SECURITY CLASSIFICATION OF REPORT Unclassified	**18. SECURITY CLASSIFICATION OF THIS PAGE** Unclassified	**19. SECURITY CLASSIFICATION OF ABSTRACT** Unclassified	**20. LIMITATION OF ABSTRACT** UL

NSN 7540-01-280-5500 Standard Form 298 (Rev. 2-89)
Prescribed by ANSI Std. 239-18

THIS PAGE INTENTIONALLY LEFT BLANK

Approved for public release; distribution is unlimited

MULTI-SCALE ANALYSIS OF A 2/2-TWILL WOVEN FABRIC COMPOSITE

Kevin K. Roach
Lieutenant, United States Navy
B.S. Mechanical Engineering, University of Texas at Austin, 1995

Submitted in partial fulfillment of the
requirements for the degrees of

MECHANICAL ENGINEER
and
MASTER OF SCIENCE IN MECHANICAL ENGINEERING

from the

NAVAL POSTGRADUATE SCHOOL
March 2002

Author: Kevin K. Roach

Approved by: Young W. Kwon, Thesis Advisor

Terry R. McNelly, Chairman
Department of Mechanical Engineering

THIS PAGE INTENTIONALLY LEFT BLANK

ABSTRACT

A micro-mechanical unit-cell model was developed for 2/2-twill woven fabric composites. A multi-scale bi-directional micro/macro-mechanical analysis technique was applied to the model in an effort to estimate effective material properties of 2/2-twill composites and decompose the effective stresses (strains) of the woven fabric composite into the stresses (strains) of the tows. When this unit-cell model is incorporated into the multi-scale analysis by combining with previously developed modules, the residual strength and stiffness of a laminated structure made of 2/2-twill woven fabric composites can be predicted along with damage progression in the structure. Damage is described at the basic material units of the composite structure, the fibers and matrix. The unit-cell model and the multi-scale analysis were validated by comparing their predicted results to available data in open literature and data obtained from a finite element models.

THIS PAGE INTENTIONALLY LEFT BLANK

TABLE OF CONTENTS

THIS PAGE INTENTIONALLY LEFT BLANK

LIST OF FIGURES

THIS PAGE INTENTIONALLY LEFT BLANK

LIST OF TABLES

THIS PAGE INTENTIONALLY LEFT BLANK

ACKNOWLEDGMENTS

Thank you to Professor Young W. Kwon for his mentorship in the completion of this research. His guidance has kept me on track and made this experience both challenging and rewarding.

My most sincere appreciation is owed my loving wife Diane, whose unconditional love and unwavering support are as much a part of my success as anything I have done in the classroom or in the fleet.

THIS PAGE INTENTIONALLY LEFT BLANK

I. INTRODUCTION

A. BACKGROUND

Composites afford engineers the unique ability to tailor material properties to specific applications. By combining two or more constituent materials, a resultant can be manufactured with varying mechanical and thermal properties. This resultant is not a solution, but two or more separate material as the constituents retain their identities in the composites. The constituents' reduced specific weight to strength ratios, increased or decreased stiffness, targeted coefficients of thermal expansion, and increased toughness are but a few of the advantages to composites. Often the advantages are manifested in cost savings due to lighter materials, increased fatigue life, and increased reliability.

Composite materials are being used increasingly in all facets of life. The ever-increasing need for lightweight, strong, and inexpensive materials is driving this increased use. These materials are filling niches in the automotive industries by providing lightweight, strong alternative to steels and aluminums in an effort to increase fuel efficiency. Additionally, these materials can be designed to be highly corrosion resistant, thus increasing the average life of automobiles. Composites are being used in military applications ranging from lightweight weaponry and body armor to shipboard superstructure applications. The aerospace industry use composites not only for the strength to weight properties to increase payload capacity but also for it thermal and mechanical properties in extreme environments. An example is the shielding tiles used to protect the space shuttle upon atmosphere reentry. The medical community use composites in the hostile environment that is the human body. Still, other industries use composites for their increased resistance to high temperature creep in applications such as turbine blades.

One of the most widely used composites is the woven fabric. Fabrics are formed by weaving continuous fibers in a predetermined pattern and then impregnating the weave with a second material to form the composite. In general the fibers, also called reinforcements, are the stiffer components while the second material is the more compliant. The compliant material will be referred to as the matrix. Weaves generally

consist of two sets of interlaced fiber bundles or tows. These bundles are called the warp and fill. The warp will be considered the horizontal bundle while the fill will be considered the vertical bundle.

Weaves patterns are defined by the repeating patterns in the warp and fill directions using the variables $\left(n_g^F\right)$ and $\left(n_g^W\right)$. They represent the n'th threads with which an orthogonal thread is interlaced. For example a warp thread is interlaced with every $\left(n_g^F\right)^{'th}$ fill thread and a fill thread is interlaced with every $\left(n_g^F\right)^{'th}$ warp thread.

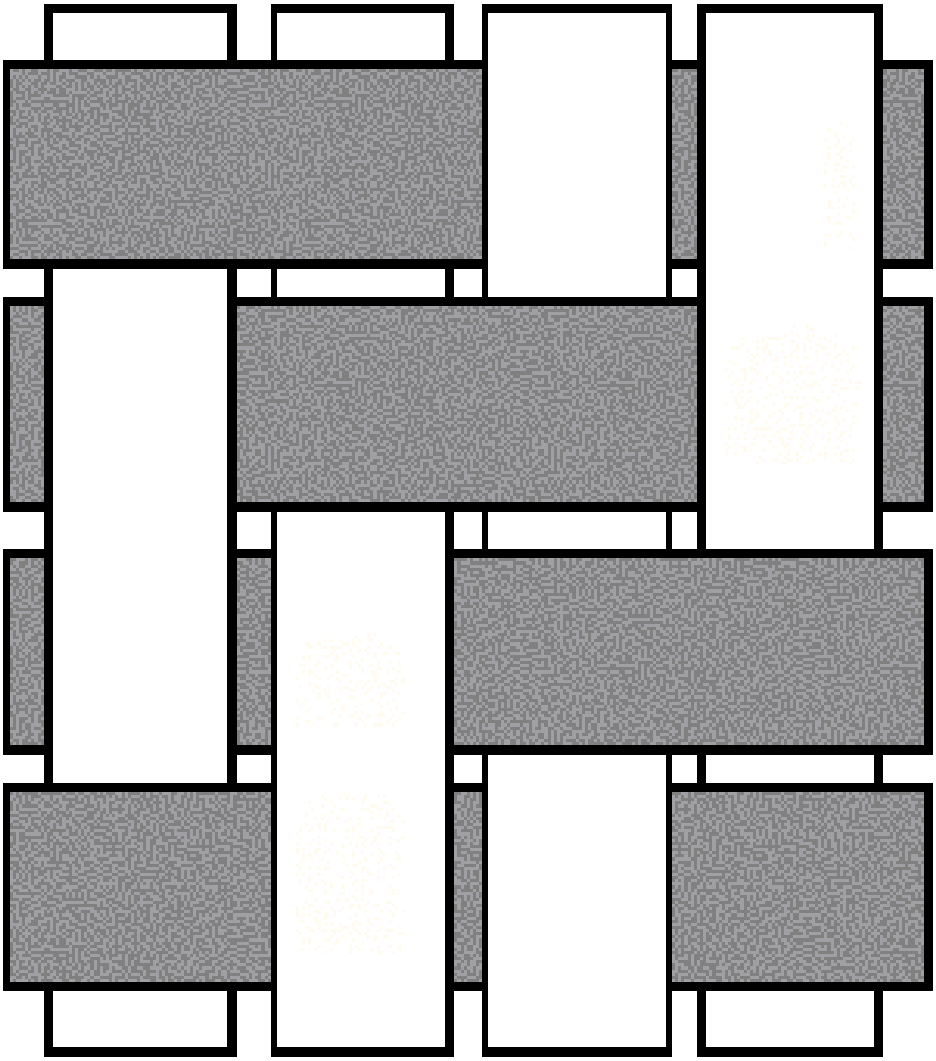

Figure 1. 2/2-Twill Composite Hybrid Model

If the weaves are such that the same fiber is used in both the warp and fill direction and $\left(n_g^F\right)=\left(n_g^W\right)$, the result is a composite with orthotropic material properties**.** Woven fabrics, however, often have different types of thread for the warp and fill bundles. These composites are known as hybrids. A 2/2-twill hybrid composite is illustrated in Figure 1.

The mechanical properties of continuous fiber composite strands are directional. In traditional continuous fiber laminated composites, all fibers lie in the same plane. This provides very desirable increases in the in-plane mechanical properties, but little in the transverse mechanical properties. Alternatively, woven fabrics composites provide mechanical improvements in both the in-plane and transverse plane directions. To take full advantage of these composites requires an efficient method to accurately predict their effective stiffnesses and strengths.

B. OBJECTIVES

The objective of this study was to develop a unit-cell model for a 2/2-twill woven fabric continuous strand composites and introduce it into a multi-level, multi-scale analysis technique for the purposes of predicting the effective stiffness and strength of the composite structures. Additionally the model was applied to a series of programs designed to predicting progressive damages in these structures. In working towards these ends a finite element model of the unit cell was developed using the MSC PATRAN/NASTRAN® commercial software packages. This model was used at the outset of the project to validate simplifying assumptions of the unit cell model and was later used to test the micro-level accuracy of the unit cell model. The woven fabric unit cell as well as a composite structure was analyzed under different in-plane loading conditions to test macro-level accuracy. All the damages in the unit cell model are described at the fiber and matrix material levels.

C. LITERARY SURVEY

There has been extensive research in the area of woven fabric composites and some is discussed here. Ishikawa and Chou [1] conducted some of the earliest research and proposed three models for estimating properties of elastic materials. Their first, the

mosaic model, bounded the elastic modulus by using various simplifying assumptions. However, this model did not account for any fiber undulation. Their second model, the fiber undulation model, addressed the undulation in continuous fiber composite in only one direction. Thus both of these two methods were largely one-dimensional analysis and could not account for interactions between the cross-plies. This led to their third model, the bridging model, which addressed the interaction between the undulation region and its surroundings.

Zhang and Harding [2] suggested an approach using a strain energy method coupled with finite element analysis. As in Ishikawa and Chou's second method, this method's principle drawback was that undulation was accounted for in only one direction. Naik and Shembekar [3] expanded the fiber undulation model to include undulation in two directions and thus the in-plane prediction of elastic moduli was said to very closely bound experimental results. Later Naik and Ganesh [4] suggested the slice array model and the element array model. In both these models, the unit cell was sliced and the elastic property in each slice was recombined to determine the overall material property. These approaches were mainly applied to simple plane weave composites under in-plain loads and close correlations were reported between experimental and numerical results.

Cox *et al.* [5], Thompson and Criffin [6], and Whitcomb and Srirengan [7] suggested three-dimensional finite element models. The major drawback of these analyses is the large computational cost of the analysis for a simple structure. These models are touted to be able to determine accurate local effects.

A number of studies have been conducted to determine the effective material properties from the fiber/matrix materials and geometry. The vast majority considers only determining the composite properties from the constituent material level and not the opposite. Examples include the MESOTEX model of Scida *et al*. [8], the CLT based model of Chaphalkar and Kelkar [9], and the model of Ng *et al.* [10].

A small number of studies have considered the decomposition of laminate strains and stress into the fiber and matrix level stresses to predict failure or damage of constituent materials. In particular, the work of Kwon et al. [11-14] used bi-directional

approach. It consists of a macro unit cell model that relates the strands to the weaves and a finite element model that relates the weaves and the structures. This model is thought to be more efficient than the model of Garnich and Hansen [15], which suggested a bi-directional model that incorporated a finite element analysis to compute the effective composite material properties from constituents' properties. Other models, such as Pechold and Rahman [16] used the simple strength of material approach, neglecting Poisson's effect.

THIS PAGE LEFT INTENTIONALLY BLANK

II. ANALYSIS TECHNIQUES AND MODELS

A. MULTI-SCALE TECHNIQUE

The basic framework of the multi-scale micro/macro-mechanical model was developed previously and applied to particulate, continuous uni-directional fiber, and plain weave composites. Here the approach is extended to 2/2-twill woven fabric composites. A brief description of the method is included here for completeness.

The model consists of three interconnected modules as shown in Figure 2. The three modules are the *fiber-strand module*, *strand-fabric module*, and *lamination module*. Using these modules, progressive damage in a laminated 2/2-twill woven fabric composite structure can be described at the fiber and matrix material level, the basic units of the structure. Damage can be classified as matrix damage, fiber breakage, and interface de-bonding. The effects of damage can be simulated at the composite structural level. In other words, residual strength and stiffness of a composite structure can be predicted based on the progressive damage at the fiber and matrix level.

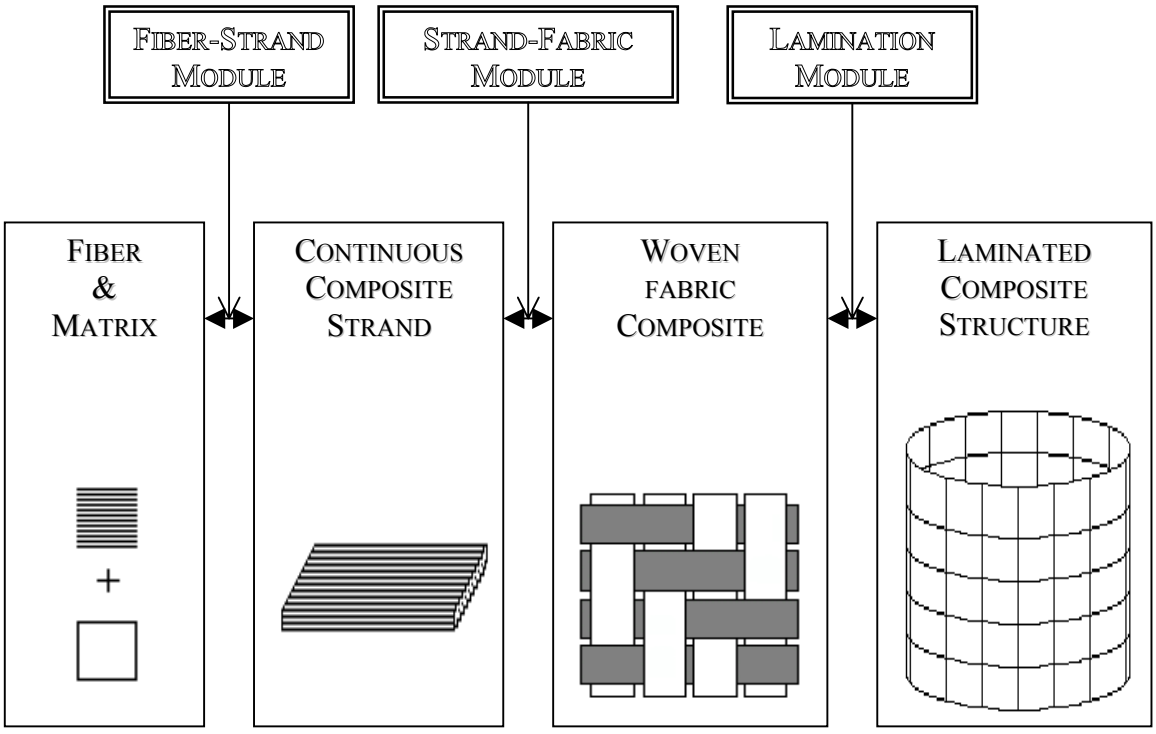

Figure 2. Multi-Level and Multi-Scale Analysis Schematic

1. Fiber-Strand

The fiber-strand module relates the constituent materials, e.g. the fiber and matrix, to the unidirectional composite strand. This module serves to determine the effective material properties of the strand from those of the constituent materials. In addition, it also decomposes the stresses and strains of the strand into fiber/matrix stresses and strains so that damage criteria can be applied to the fiber/matrix level.

This module was developed using a unit-cell with four sub-cells. One of the sub-cells represents the fiber and the other three denote the matrix. Within each sub-cell, stresses and strains are assumed to be uniform. In order to develop the mathematical equation of the fiber-strand module, the following equations are solve together: equilibrium at the interfaces of sub-cell, deformation compatibility among sub-cells, the volume average of sub-cells, and the constitutive equations of each sub-cell. Then, the resultant equations are summarized below:

$$[E^{str}] = [V][E][R_2] \quad \textbf{(1)}$$

$$\{\varepsilon^{\alpha}\} = [R_2]\{\varepsilon^{str}\} \quad \textbf{(2)}$$

where $[E^{str}]$ is the effective material property matrix for the composite strand, $[V]$ is the matrix containing volume fractions of each sub-cell, $[E]$ is the matrix of material properties of the constituents, and $[R_2]$ is the decomposition matrix that transforms strand strains $\{\varepsilon^{str}\}$ into the fiber and matrix strains $\{\varepsilon^{\alpha}\}$. Detailed development of these two expressions, which provide the bi-directional passage, was discussed in previous studies [11,12].

Once fiber and matrix stresses are computed, failure criteria are applied to the stresses. For the fiber breakage criterion, the normal stress along the fiber orientation does not exceed the strength of the fiber material. Usually, different strength values are used for tensile and compressive loads, respectively, in consideration of fiber buckling. The matrix material uses an isotropic failure criterion like the maximum shear stress criterion as long as the material is considered as isotropic. If there is failure in fiber and/or matrix material(s), the material properties like elastic modulus are degraded so as

to include the failure effects. Then, the degraded material properties are used in the fiber-strand module to compute the effective properties of the locally failed strands.

2. Strand-Fabric

The strand-fabric module relates effective material properties of a unidirectional composite strand to those of a 2/2-twill woven fabric. The module also decomposes the woven fabric stresses and strains into strand stresses and strains. In order to perform these functions, a unit-cell model is developed as described later.

3. Lamination

The lamination module relates the effective material properties of a woven fabric lamina to the laminated properties of multiple layers. These properties are used in the finite element analysis of a laminated structure made of a 2/2-twill woven fabric composite. Once the deformations, stresses, and strains are computed for the laminated composite structure, the module computes the stresses and strains of each lamina of the composite structure. In order to undertake these functions, the lamination theory is used. Either the classical lamination theory or a higher order theory may be used in the module. In this study, the classical theory available in most textbooks was used so that it was not presented here.

B. MULTI-SCALE MICRO/MACRO ANALYSIS

The procedure of the multi-scale micro/macro analysis is presented. The analysis was derived for a laminated woven fabric composite structure and uses the 2/2-twill composites unit cell to link between the laminated structure and the constituent materials.

1. Compute effective material properties of tows (unidirectional strand) in the matrix using the *fiber-strand* module, the material properties of fibers and matrix, and their volume fractions.
2. Compute effective properties of the 2/2-twill woven fabric unit cell laminar from the material properties of the unidirectional strand and the geometry of the weave using the *strand-fabric* module.
3. Calculate effective properties of a laminated woven fabric composite from the property of each laminar and its orientation using the *lamination* module.
4. Apply a load to the structure and determine the deformation, stresses, and strains from a finite element model using the material properties obtained in the previous step.
5. Compute the strains (stresses) at each lamina from the deformation determined at the laminated structural analysis using the *lamination* module.

6. Decompose the strains (stresses) at a lamina into the strains (stresses) at the unidirectional strands using the *strand-fabric* module.
7. Decompose the strains (stresses) at the unidirectional strand into the strains (stresses) in the fiber and the matrix using the *fiber-strand* module.
8. Apply damage (failure) criteria to determine initiation of new damage or progression of existing damage at the fiber and matrix level.
9. Once there is new damage or progression of damage at the fiber and matrix level, the degraded properties of the unidirectional strand are computed depending on the damage mode and state using the *fiber-strand* module.
10. Repeat steps 2 through 9 until either the ultimate failure of the composite structure or the final load applied to the structure.

C. 2/2-TWILL UNIT CELL MODELS

Figure 3 and Figure 4 represent a 2/2-twill woven fabric composite lamina and repeating unit-cell respectively. Two analytical models were created for the twill composite, a finite element model utilizing commercial finite element software and a mathematical model referred to as the Unit Cell model.

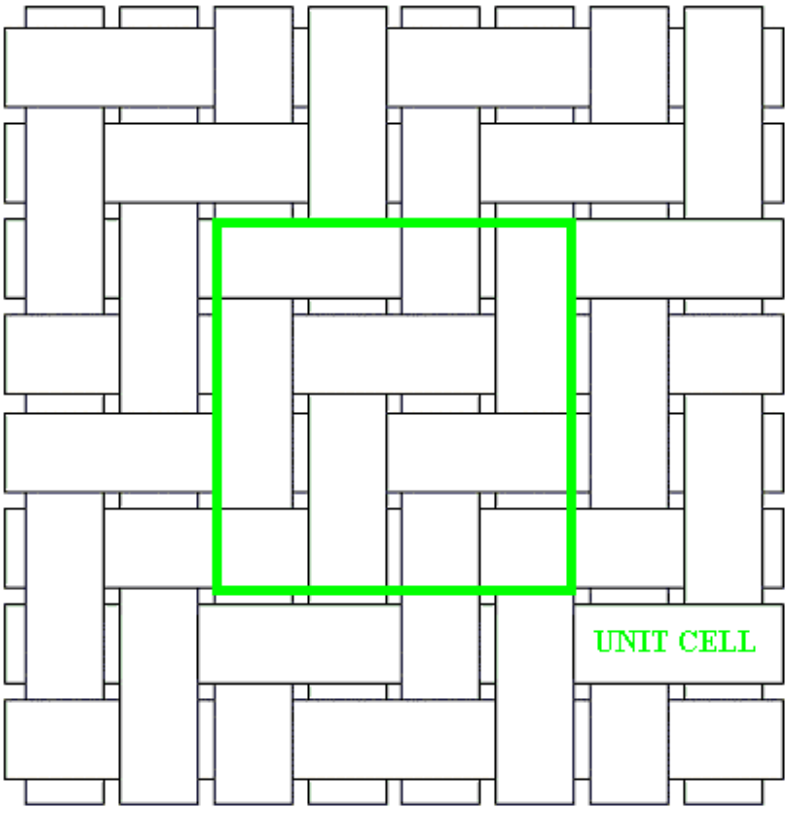

Figure 3. 2/2-Twill Composite Lamina

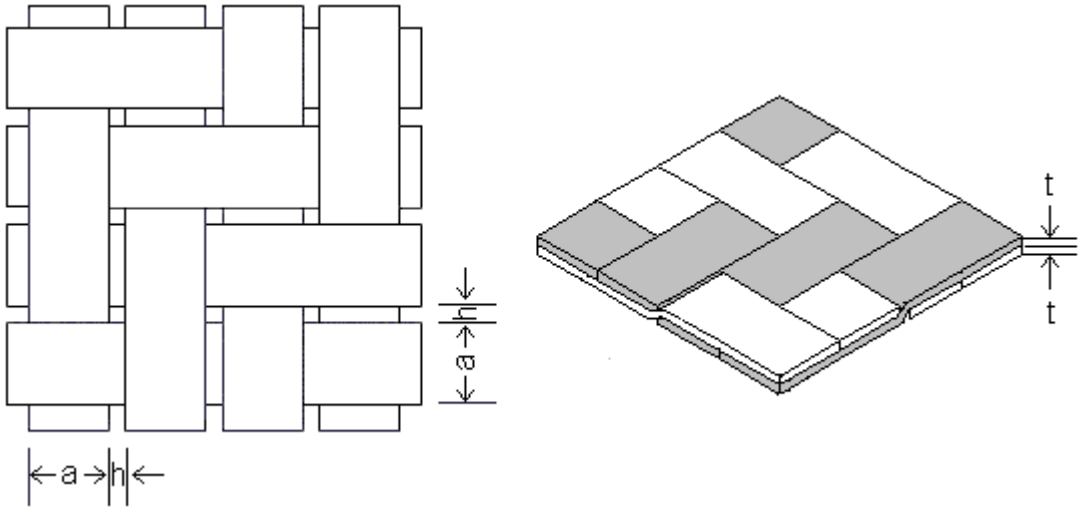

Figure 4. 2/2-Twill Composite Unit-Cell

1. Finite Element Model

The finite element cell was created using the MSC PATRAN/NASTRAN® commercial software. The model was designed using 13456 wedge shaped elements and 8585 nodes and represents a single repeating unit of the 2/2-twill lamina. A wedge shaped element and the full finite element mesh are presented in Figure 5 and Figure 6, respectively.

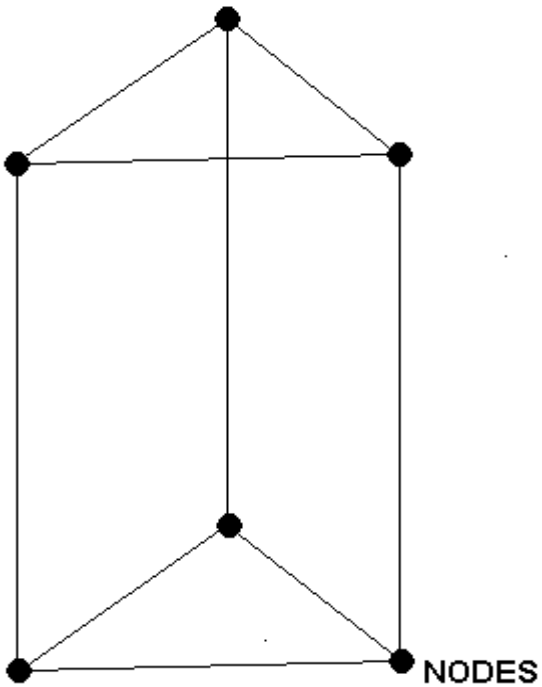

Figure 5. Wedge Shaped Finite Element

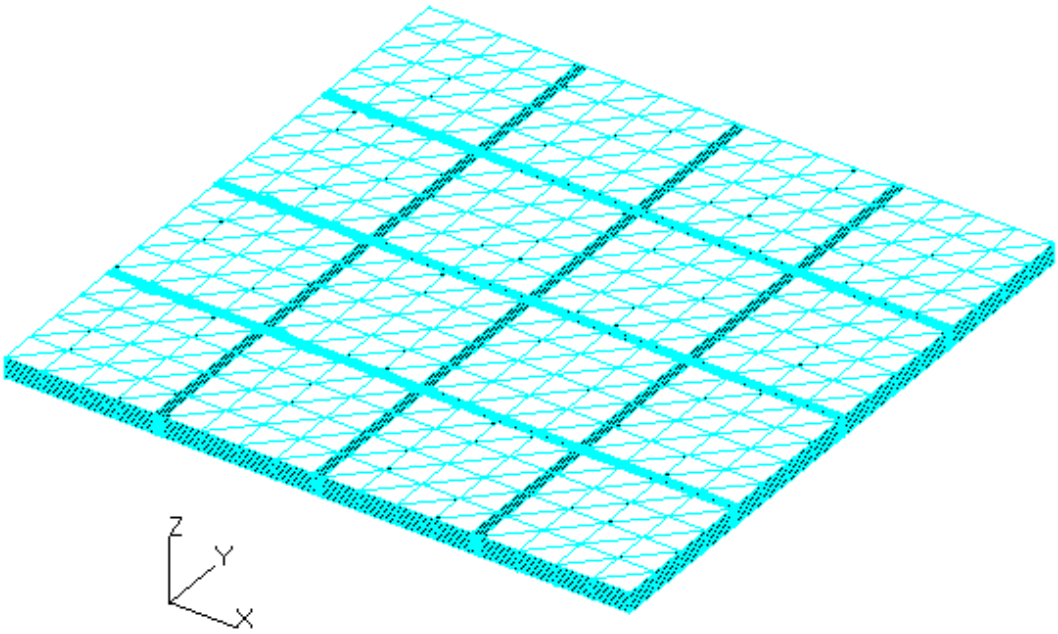

Figure 6. Finite Element Mesh of Repeating Cell

Orthotropic material properties were applied to the vertical and horizontal strands in plane in the weave along the local coordinate axes. Figure 7 illustrates the strand fiber direction. The strand direction corresponds to the 1-direction in the local coordinate system. Not depicted are the strand directions for the undulated sections of the weave. Orthotropic material properties were applied to these sections with the local coordinate 1-direction corresponding to their undulation angles. The darker squared areas and all other voids were filled with the isotropic matrix material.

The finite element model was instrumental in validating both the assumptions of and results from the unit cell model. For the purposes of validating initial assumptions, the finite element model was subjected to a uniformed displacement along the y direction with symmetric boundary conditions applied at x, y, and z = 0 planes. The fringe plot of the finite element model with symmetric boundary conditions and uniformed displacement in the y direction is shown in Figure 8.

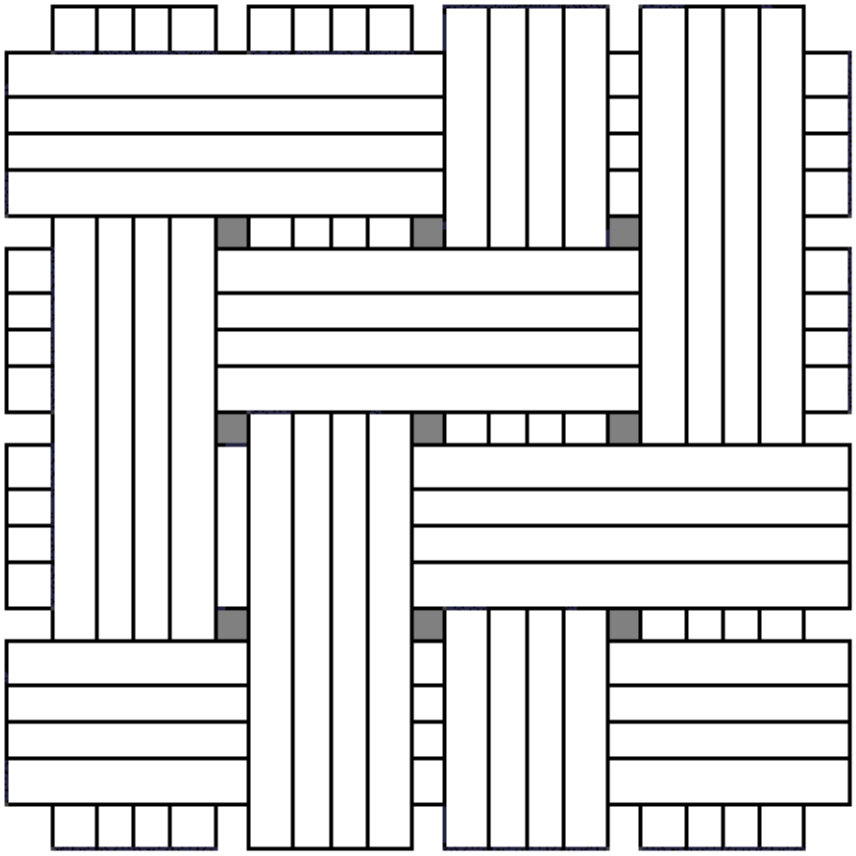

Figure 7. Material Properties Illustration

2. Unit Cell model

The unit cell model was designed so the micro-macro technique could be applied to it. The unit cell model makes the following assumptions:

a. The stress state remains in the elastic regime
b. The matrix is defect free
c. No residual stresses are present in the lamina
d. Fibers are uniformly distributed in the matrix
e. Perfect bonding occurs at the matrix- fiber interface
f. The composite strands are orthotropic.
g. Each sub-cell has a constant stress states.
h. Subcells that have the equivalent boundary conditions and material properties will have equivalent stress states.
i. The unit cell is constrained such that the no curvature results due to the inherent force-moment coupling of the composite strands.

The unit cell was divided into 77 sub-cells. Of the 77 sub-cells, some were theorized to have the same average stress states. The finite element model was run on several materials under a uniformed displacement to validate this assumption. Figure 9 is a fringe plot of the unit cell stress state under a uniform deformation. This plot is provided as a visual aid for the reader, not as definitive proof of certain cells having the same average stress states. Figure 10 is a schematic depiction of the sub-cells. Those having the same number designation are assumed to have the same average stress state.

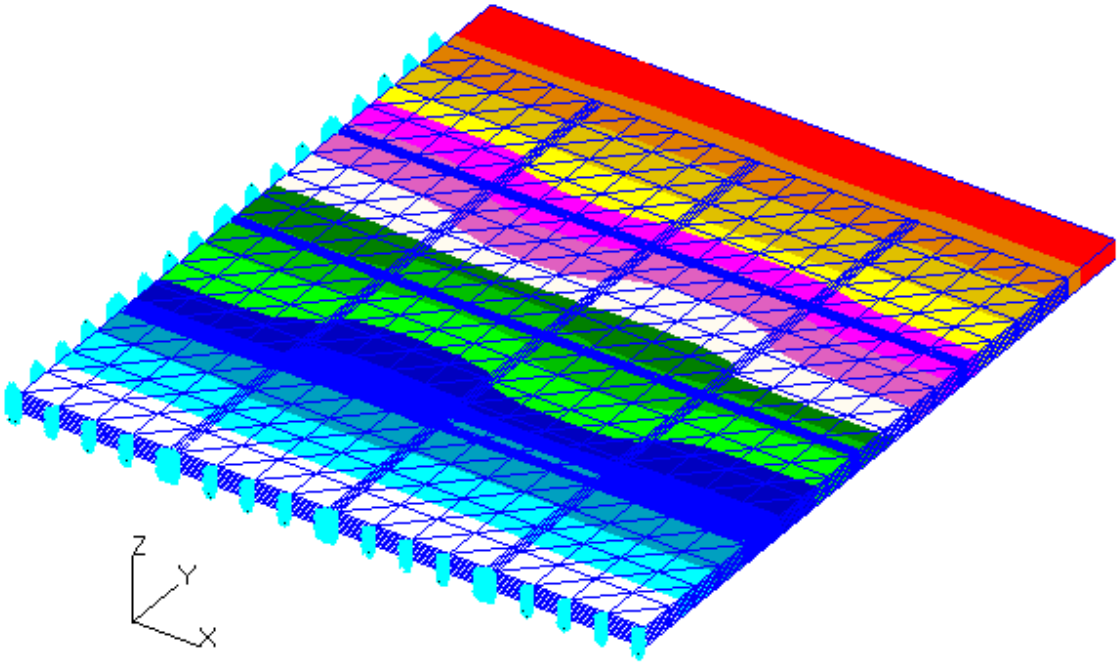

Figure 8. Uniformed Displacement Finite Element Fringe Plot

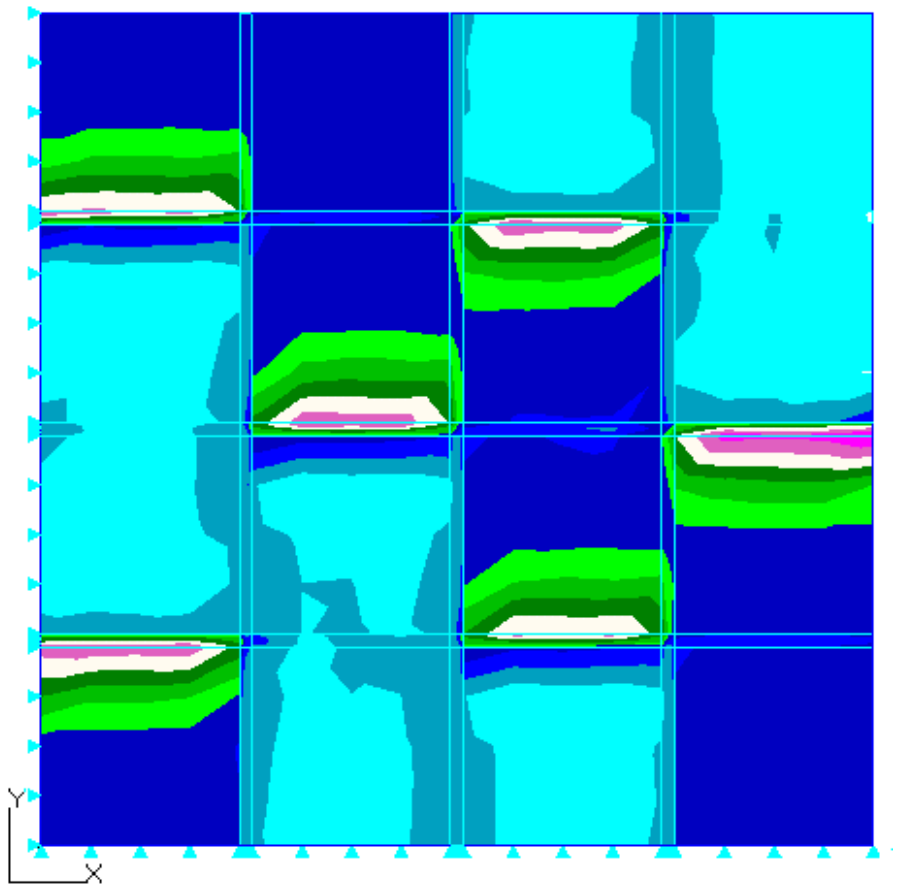

Figure 9. Stress State Fringe Plot for Uniformed Displacement

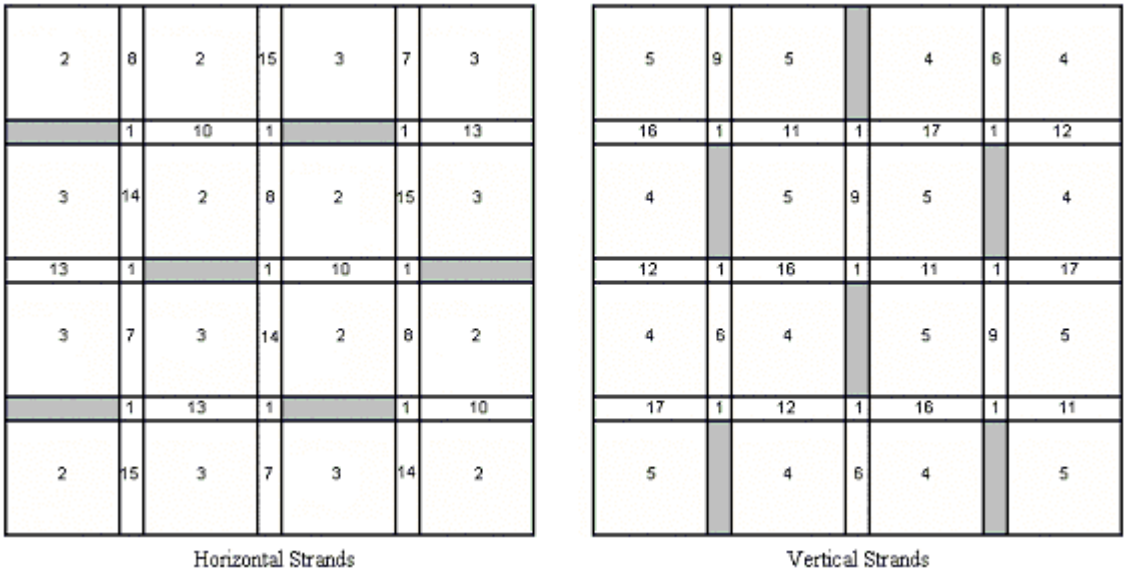

Figure 10. Sub-cell Numbering

As a result, 17 independent sub-cells are used in the unit cell model. Forty-eight linearly independent equations were developed which relate the normal stresses and normal strains of the 17 uniquely stressed sub-cells. These 48 equations are the basis for the unit cell model. The average stress and strain of each sub-cell are used in all the subsequent equations. The first set of equations represents the stress equilibrium at the sub-cells interfaces. Applying equilibrium to any two neighboring sub-cells results in the following normal stress equations, where the subscripts indicate stress components and the superscripts designate the sub-cell numbers. Equations (3), (4), and (5) are a set of normal stress equilibriums in the 1-, 2-, and 3-directions respectively.

$$\begin{aligned}
&\sigma_{11}^{2}=\sigma_{11}^{8};\quad \sigma_{11}^{2}=\sigma_{11}^{15};\quad \sigma_{11}^{2}=\sigma_{11}^{14};\quad \sigma_{11}^{3}=\sigma_{11}^{7};\quad \sigma_{11}^{3}=\sigma_{11}^{15};\\
&\sigma_{11}^{3}=\sigma_{11}^{14}\quad \sigma_{11}^{5}=\sigma_{11}^{9};\quad \sigma_{11}^{4}=\sigma_{11}^{6};\quad \sigma_{11}^{1}=\sigma_{11}^{16};\quad \sigma_{11}^{1}=\sigma_{11}^{17};\\
&\sigma_{11}^{1}=\sigma_{11}^{10}+\sigma_{11}^{11};\quad \sigma_{11}^{1}=\sigma_{11}^{12}+\sigma_{11}^{13};
\end{aligned} \tag{3}$$

$$\begin{aligned}
&\sigma_{22}^{4}=\sigma_{22}^{16};\ \sigma_{22}^{4}=\sigma_{22}^{17};\quad \sigma_{22}^{4}=\sigma_{22}^{12};\quad \sigma_{22}^{5}=\sigma_{22}^{17};\quad \sigma_{22}^{5}=\sigma_{22}^{17};\\
&\sigma_{22}^{5}=\sigma_{22}^{11}\quad \sigma_{22}^{3}=\sigma_{22}^{13};\quad \sigma_{22}^{2}=\sigma_{22}^{10};\quad \sigma_{22}^{1}=\sigma_{22}^{14};\quad \sigma_{22}^{1}=\sigma_{22}^{15};\\
&\sigma_{22}^{1}=\sigma_{22}^{6}+\sigma_{22}^{7};\quad \sigma_{22}^{1}=\sigma_{22}^{8}+\sigma_{22}^{9};
\end{aligned} \tag{4}$$

$$\begin{aligned}
&\sigma_{33}^{2}=\sigma_{33}^{5};\quad \sigma_{33}^{3}=\sigma_{33}^{4};\quad \sigma_{33}^{6}=\sigma_{33}^{7};\\
&\sigma_{33}^{8}=\sigma_{33}^{9};\quad \sigma_{33}^{10}=\sigma_{33}^{11}\quad \sigma_{33}^{12}=\sigma_{33}^{13};
\end{aligned} \tag{5}$$

Equations (6) through (14) represent the directional strain compatibility assuming a uniform deformation of the unit-cell, where *a* and *h* are the dimensions of the fill and warp strands of the composite material shown in Figure 4.

$$\begin{aligned}
&2a\left(\varepsilon_{11}^{2}+\varepsilon_{11}^{3}\right)+h\left(\varepsilon_{11}^{7}+\varepsilon_{11}^{8}\right)=2a\left(\varepsilon_{11}^{4}+\varepsilon_{11}^{5}\right)+h\left(\varepsilon_{11}^{6}+\varepsilon_{11}^{9}\right)\\
&2a\left(\varepsilon_{11}^{2}+\varepsilon_{11}^{3}\right)+h\left(\varepsilon_{11}^{8}\right)=2a\left(\varepsilon_{11}^{4}+\varepsilon_{11}^{5}\right)+h\left(\varepsilon_{11}^{9}\right)\\
&2a\left(\varepsilon_{11}^{2}+\varepsilon_{11}^{3}\right)+h\left(\varepsilon_{11}^{8}+\varepsilon_{11}^{14}+\varepsilon_{11}^{15}\right)=a\left(\varepsilon_{11}^{10}+\varepsilon_{11}^{13}+\varepsilon_{11}^{16}+\varepsilon_{11}^{17}\right)+3h\left(\varepsilon_{11}^{1}\right)\\
&\varepsilon_{11}^{10}+\varepsilon_{11}^{12}=\varepsilon_{11}^{11}+\varepsilon_{11}^{13}
\end{aligned} \tag{6}$$

$$
\begin{aligned}
&2a\left(\varepsilon_{22}^{2}+\varepsilon_{22}^{3}\right)+h\left(\varepsilon_{22}^{11}+\varepsilon_{22}^{12}\right)=2a\left(\varepsilon_{22}^{4}+\varepsilon_{22}^{5}\right)+h\left(\varepsilon_{22}^{10}+\varepsilon_{22}^{13}\right)\\
&2a\left(\varepsilon_{22}^{2}+\varepsilon_{22}^{3}\right)+h\left(\varepsilon_{22}^{13}\right)=2a\left(\varepsilon_{22}^{4}+\varepsilon_{22}^{5}\right)+h\left(\varepsilon_{22}^{12}\right)\\
&2a\left(\varepsilon_{22}^{4}+\varepsilon_{22}^{5}\right)+h\left(\varepsilon_{22}^{12}+\varepsilon_{22}^{16}+\varepsilon_{22}^{17}\right)=a\left(\varepsilon_{22}^{6}+\varepsilon_{22}^{9}+\varepsilon_{22}^{14}+\varepsilon_{22}^{15}\right)+3h\left(\varepsilon_{22}^{1}\right)\\
&\varepsilon_{22}^{6}+\varepsilon_{22}^{8}=\varepsilon_{22}^{7}+\varepsilon_{22}^{9}
\end{aligned}
\qquad \textbf{(7)}
$$

$$
\begin{aligned}
&\varepsilon_{33}^{2}+\varepsilon_{33}^{5}=\varepsilon_{33}^{16};\quad \varepsilon_{33}^{2}+\varepsilon_{33}^{5}=\varepsilon_{33}^{15};\quad \varepsilon_{33}^{2}+\varepsilon_{33}^{5}=\varepsilon_{33}^{17};\quad \varepsilon_{33}^{2}+\varepsilon_{33}^{5}=\varepsilon_{33}^{14};\\
&\varepsilon_{33}^{2}+\varepsilon_{33}^{5}=\varepsilon_{33}^{1};\quad \varepsilon_{33}^{2}+\varepsilon_{33}^{5}=\varepsilon_{33}^{6}+\varepsilon_{33}^{7};\quad \varepsilon_{33}^{2}+\varepsilon_{33}^{5}=\varepsilon_{33}^{12}+\varepsilon_{33}^{13};\\
&\varepsilon_{33}^{2}+\varepsilon_{33}^{5}=\varepsilon_{33}^{6}+\varepsilon_{33}^{8};\quad \varepsilon_{33}^{2}+\varepsilon_{33}^{5}=\varepsilon_{33}^{10}+\varepsilon_{33}^{11};\quad \varepsilon_{33}^{2}+\varepsilon_{33}^{5}=\varepsilon_{33}^{3}+\varepsilon_{33}^{4}
\end{aligned}
\qquad \textbf{(8)}
$$

The constitutive equation for each sub-cell is given below in Equation (15), where $(\sigma_{ij}^{str})^{n}$ and $(\varepsilon_{kl}^{str})^{n}$ are the n^{th} sub-cell stresses and strains, and $(E_{ijkl}^{str})^{n}$ is the sub-cell material property matrix in terms of the unit-cell axes.

$$(\sigma_{ij}^{str})^{n}=(E_{ijkl}^{str})^{n}(\varepsilon_{kl}^{str})^{n} \qquad \textbf{(9)}$$

The stiffness matrix, $(E_{ijkl}^{str})^{n}$, is determined from stress and strain equations in conjunction with the proper transformation matrices.

3. Coordinate Transformation

A result of weaving is that fibers must be undulated. The undulation angle is measured from the plane in which the majority of the fibers lay straight. We consider undulation angles of 10-15 degrees for these studies. The undulated portions of the strand must have their material properties adjusted to that of the global coordinate system. A brief explanation of stiffness transformation follows.

Let coordinate system X, Y, and Z be the global coordinate system and x_1, y_1, and z_1 be the local coordinate system where the fiber in the strand of interest is aligned with local axis.

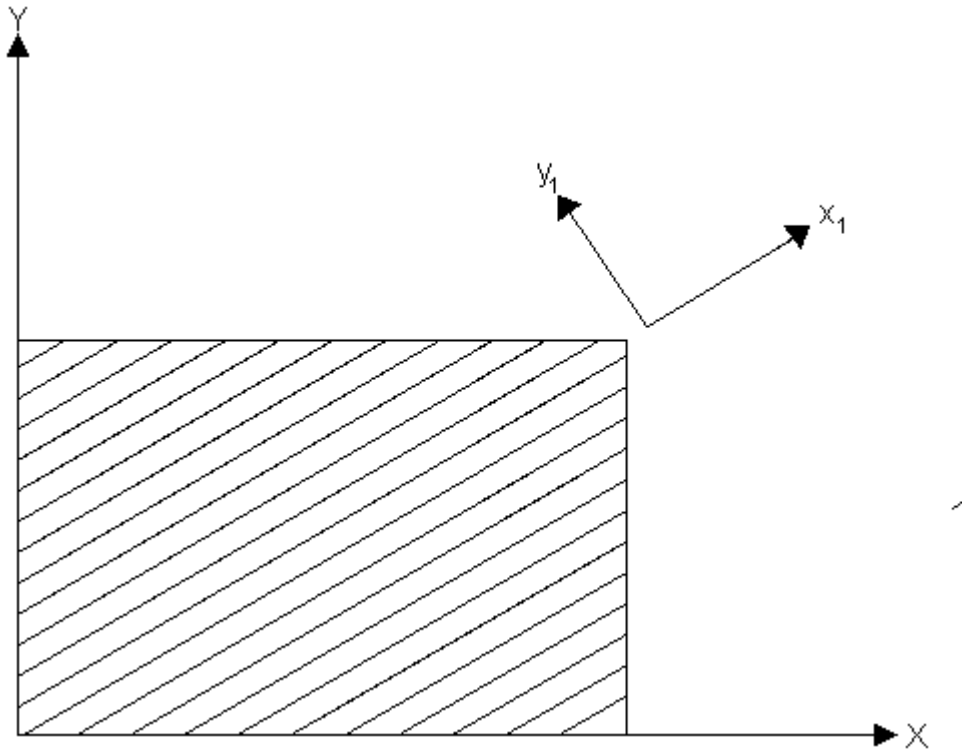

Figure 11. Coordinate Transformation Diagram

The stress and strain transformation from local coordinates to global coordinates will be:

$$\begin{aligned} \{\sigma\}^{x_1y_1z_1} &= [T_\sigma]\{\sigma\}^{xyz} \\ \{\varepsilon\}^{x_1y_1z_1} &= [T_\varepsilon]\{\varepsilon\}^{xyz} \end{aligned} \tag{10}$$

The constitutive equations are:

$$\begin{aligned} \{\sigma\}^{xyz} &= [C]^{xyz}\{\varepsilon\}^{xyz} \\ \{\sigma\}^{x_1y_1z_1} &= [C]^{x_1y_1z_1}\{\varepsilon\}^{x_1y_1z_1} \end{aligned} \tag{11}$$

Mathematical manipulation results in the following stiffness transformation equations.

$$\begin{aligned} \{\sigma\}^{x_1y_1z_1} &= [C]^{x_1y_1z_1}[T_\varepsilon]\{\varepsilon\}^{xyz} \\ [T_\sigma]\{\sigma\}^{xyz}_{kl} &= [C]^{x_1y_1z_1}[T_\varepsilon]\{\varepsilon\}^{xyz} \\ \{\sigma\}^{xyz} &= [T_\sigma]^{-1}[C]^{x_1y_1z_1}[T_\varepsilon]\{\varepsilon\}^{xyz} \\ \{\sigma\}^{xyz} &= [C]^{xyz}\{\varepsilon\}^{xyz} \end{aligned} \tag{12}$$

where

$$[C]^{xyz} = [T_\sigma]^{-1}[C]^{x_1y_1z_1}[T_\varepsilon] \tag{13}$$

Finally, the transformation matrices are as follows:

$$[T_\varepsilon]^{-1} = \begin{bmatrix} m^2 & n^2 & 0 & 0 & 0 & mn \\ n^2 & m^2 & 0 & 0 & 0 & -mn \\ 0 & 0 & 1 & 0 & 0 & 0 \\ 0 & 0 & 0 & m & -n & 0 \\ 0 & 0 & 0 & n & m & 0 \\ -2mn & 2mn & 0 & 0 & 0 & m^2-n^2 \end{bmatrix}$$

$$[T_\sigma]^{-1} = \begin{bmatrix} m^2 & n^2 & 0 & 0 & 0 & 2mn \\ n^2 & m^2 & 0 & 0 & 0 & -2mn \\ 0 & 0 & 1 & 0 & 0 & 0 \\ 0 & 0 & 0 & m & -n & 0 \\ 0 & 0 & 0 & n & m & 0 \\ -mn & mn & 0 & 0 & 0 & m^2-n^2 \end{bmatrix}$$

$$[E_{ijkl}^{str}] = [T_\sigma]^{-1}[\overline{E}^{str}][T_\varepsilon] \tag{14}$$

The matrices $[T_\sigma]$ and $[T_\varepsilon]$ are the stress and strain transformation matrices [17]. Transformation matrices account for a reduction or increase in a composite's material properties when the composite is rotated with respect to the coordinate axes from which the property was measured.

The final equations describe the relationship between the woven fabric unit-cell stresses (strains) and the strand sub-cell stresses (strains). The woven fabric unit-cell stresses and strains are computed as volumetric average of sub-cell stresses and strains.

$$\sigma_{ij}^{wf} = \sum_{n=1}^{17} V^n \left(\sigma_{ij}^{str}\right)^n \tag{15}$$

$$\varepsilon_{ij}^{wf} = \sum_{n=1}^{17} V^n \left(\varepsilon_{ij}^{str}\right)^n \tag{16}$$

where V^n is the volume fraction of the n^{th} sub-cell. After considering Equations (9) through (18), the following relationships result.

$$E_{ijkl}^{wf} = f\left((E_{ijkl}^{str})^n, a, h, t\right) \quad \textbf{(17)}$$

$$(\varepsilon_{ij}^{str})^n = g\left(\varepsilon_{ij}^{wf}, a, h, t\right) \quad \textbf{(18)}$$

These two equations provide the bi-directional passage of the strand-fabric module. Equation (19) is used to compute the effective woven fabric stiffness, E_{ijkl}^{wf}, of a 2/2-twill composite from the stiffness, $(E_{ijkl}^{str})^n$, of unidirectional strand and the weave geometric dimensions, *a*, *h*, and *t*. Additionally, Equation (18) decomposes the 2/2-twill composite strains into the sub-cell strains. The sub-cell stresses can then be calculated using Equation (9).

III. NUMERICAL MODEL VALIDATION

A. 2/2-TWILL UNIT CELL MODEL USING MULTI-SCALE ANAYLYSIS

The 2/2-twill composites were studied using the Multi-Scale *Strand-Fabric* module. Three different fiber/matrix pairs were analyzed and the resulting composite woven fabric stiffnesses were compared to published data as a means of validating both the 2/2-twill Unit Cell and the Multi-Scale analysis technique. It is worth noting that all other modules in the Multi-Scale analysis technique have been validated in previous work [11-13]. Table 1 represents the material properties for the fiber and matrix material.

	E_1 *(GPa)*	E_2, E_3 *(GPa)*	G_{12} *(GPa)*	G_{23} *(GPa)*	ν_{12}	ν_{23}	σ_{ten} *(MPa)*
S2 Glass	85.55	85.55	13.8	13.8	0.25	0.25	2700
C-50 resin	3.45	3.45	1.6	1.6	0.35	0.35	70
E-glass	73	73	30.4	30.4	0.2	0.2	2500
Epoxy	3.2	3.2	1.16	1.16	.38	.38	70
Carbon	230	24	50	33	.28	.25	3240
Bakelite	3.2	3.2	1.19	1.19	.35	.35	77

Table 1. Properties of the Constituent Materials

Tables 2 through 4 are stiffness results from both experimental and other analytical methods. Table 2 only compares stiffnesses in the x- and y-directions for the S2/C50 Woven Fabric. This is because no experimental or other analytical results were uncovered by the completion of this work. Similarly, no experimental data was available for the z-direction in Table 3 and Table 4.

In all 3 cases the absolute relative error of the presented results was less than 3%, where the absolute relative error was calculated as shown below in Equation (19).

$$abs\ rel\ error = \frac{\left|E_{\exp} - E_{pre}\right|}{E_{\exp}} \times 100\% \quad \textbf{(19)}$$

	$E_x=E_y$ *(GPa)*
Experiment [18]	28.7
Analytical [18]	30.6
Present	28.5

Table 2. Properties of the S2/C50 Woven Fabric

	$E_x=E_y$ (GPA)	E_z (GPA)
Experiment [8]	19.24	N/A
Analytical [8]	19.54	10.93
Present	19.67	9.21

Table 3. Properties of the E-Glass/Epoxy Woven Fabric

	$E_x=E_y$ (GPA)	E_z (GPA)
Experiment [19]	49.38	N/A
Analytical [19]	48.17	8.18
Present	50.3	7.52

Table 4. Properties of the Carbon/Bakelite Woven Fabric

IV. RESULTS AND DISCUSSION

A. COMPOSITE LAMINA UNDER UNIAXIAL STRESS

Progressive failure of a composite lamina under a tensile load was studied. It was expected that the first signs of failure would be cracking of matrix material in the strands oriented transverse to the loading direction. Thus, matrix material in the transverse direction to the load was degraded gradually and the reduced effective material properties were computed. Figure 12 is a plot of the normalized reduced effective modulus in the transverse direction (E_y) as a function of the progressive transverse cracking matrix modulus in the transverse direction. The progressive transverse matrix cracking was quantified as a percentage reduction in the matrix modulus in the transverse strands.

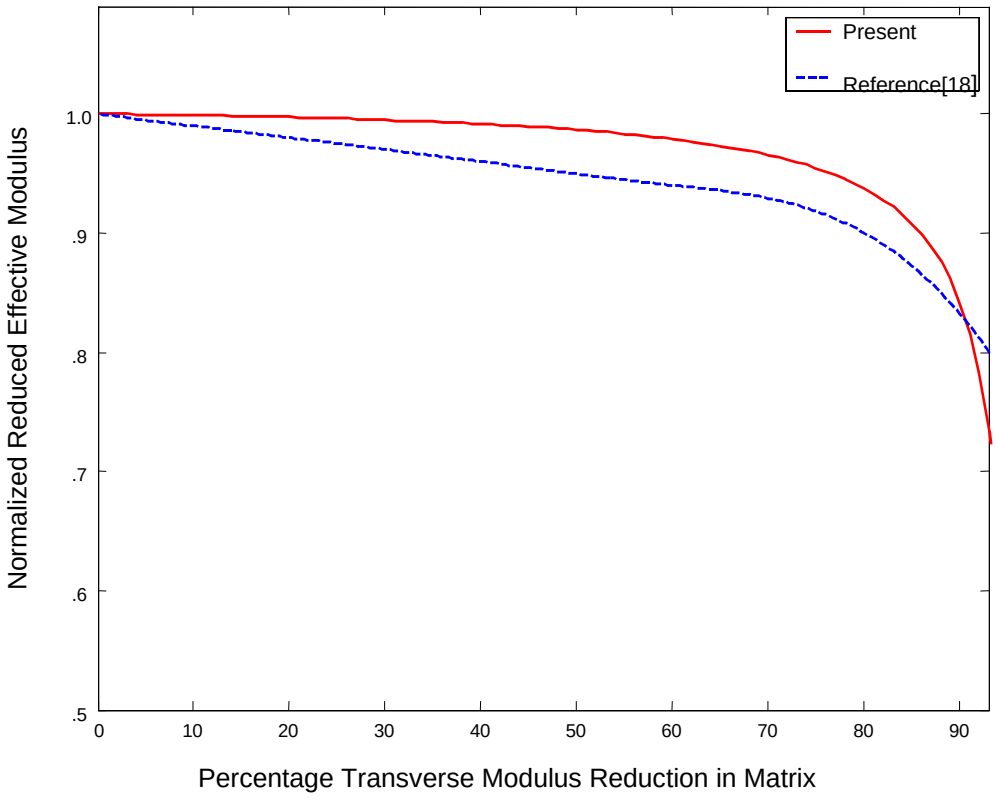

Figure 12. Effective Transverse Modulus versus Transverse Matrix Damage

The reduced modulus was normalized with respect to the virgin modulus. The plot indicates the transverse elastic modulus decreases nonlinearly with the percentage

matrix degradation. The transverse modulus is minimally affected until the matrix damage is more than 50 percent. As the percentage matrix damage becomes very high, the transverse modulus drops significantly as seen in the figure. The present prediction agreed well with that in Reference [18].

B. FLAT PLATE WITH CIRCULAR HOLE UNDER UNIAXIAL STRESS

The Multi-Scale Analysis Technique utilizing the 2/2-twill unit cell was applied to a laminated composite plate with a center-drilled hole. The objective was to determine an analytical Stress versus Strain plot and to simulate failure initiation and progression of 2/2-twill woven fabric composite plates with drilled holes at the center. Plates with three different hole sizes were considered. The hole diameters were 3 mm, 6 mm, and 9 mm.

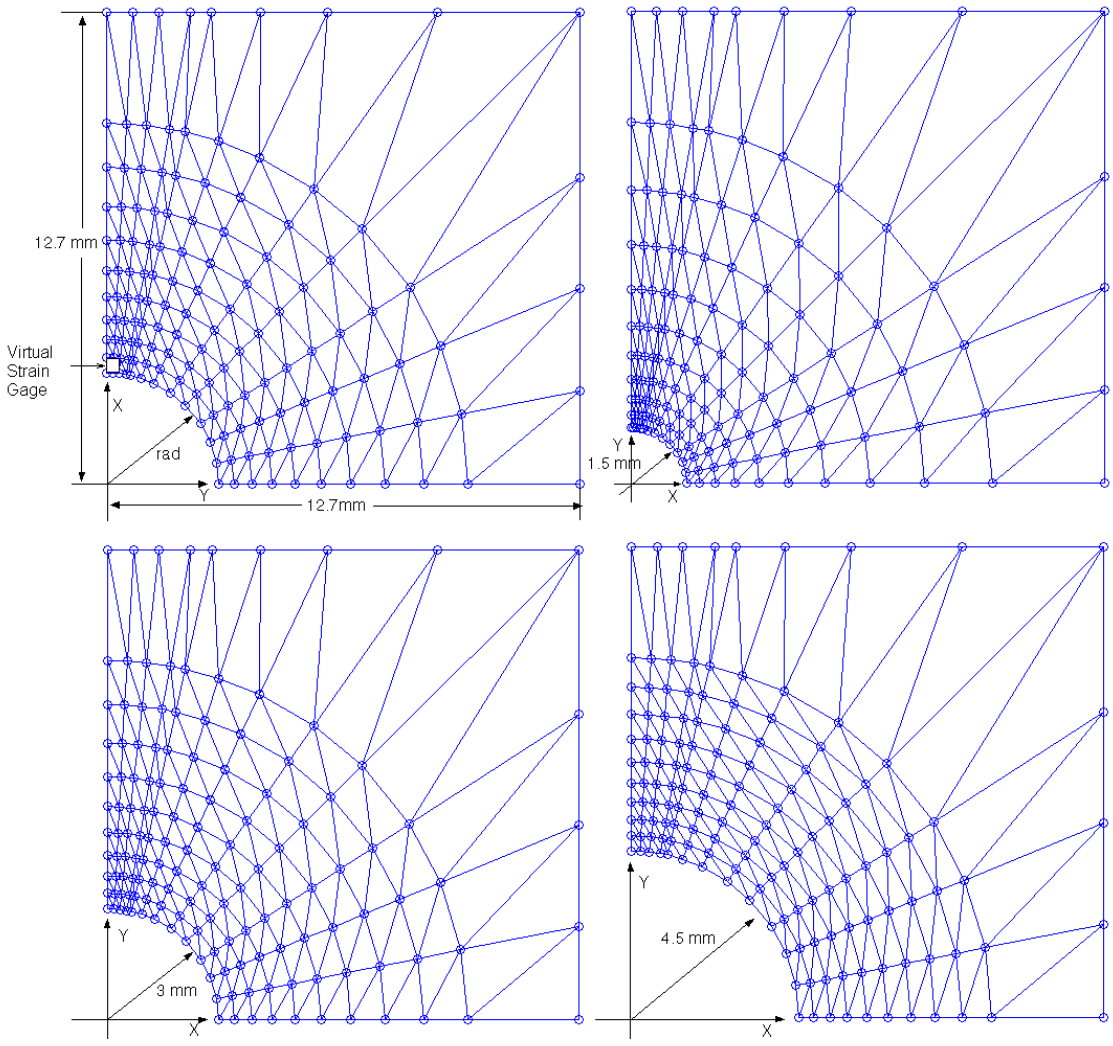

Figure 13. Finite Element Mesh of Plate Quarters with Circular Holes

A finite element model of the plates contained 143 nodes and 240 2-dimensional triangular elements. Because of symmetry, only a quarter of each plate was modeled. Figure 13 shows the finite element meshes of the plate quarters for each of the 3 hole sizes as well as a mesh model depicting dimensions. Symmetric boundary conditions were applied to the bottom and left boundaries, the inner radius was left free, and a uniform displacement was applied along the right boundary of the mesh. Figure 14 is a nodal displacement plot. The dashed lines represent the deformed plate. The strains are exaggerated for the sake of clarity. The plates represent laminated composite structure block in the Multi-Scale model shown in Figure 3. The bi-directionality of modules will allow the stresses (strains) of the composite structure to be decomposed into the stresses (strains) of the fiber and matrix materials.

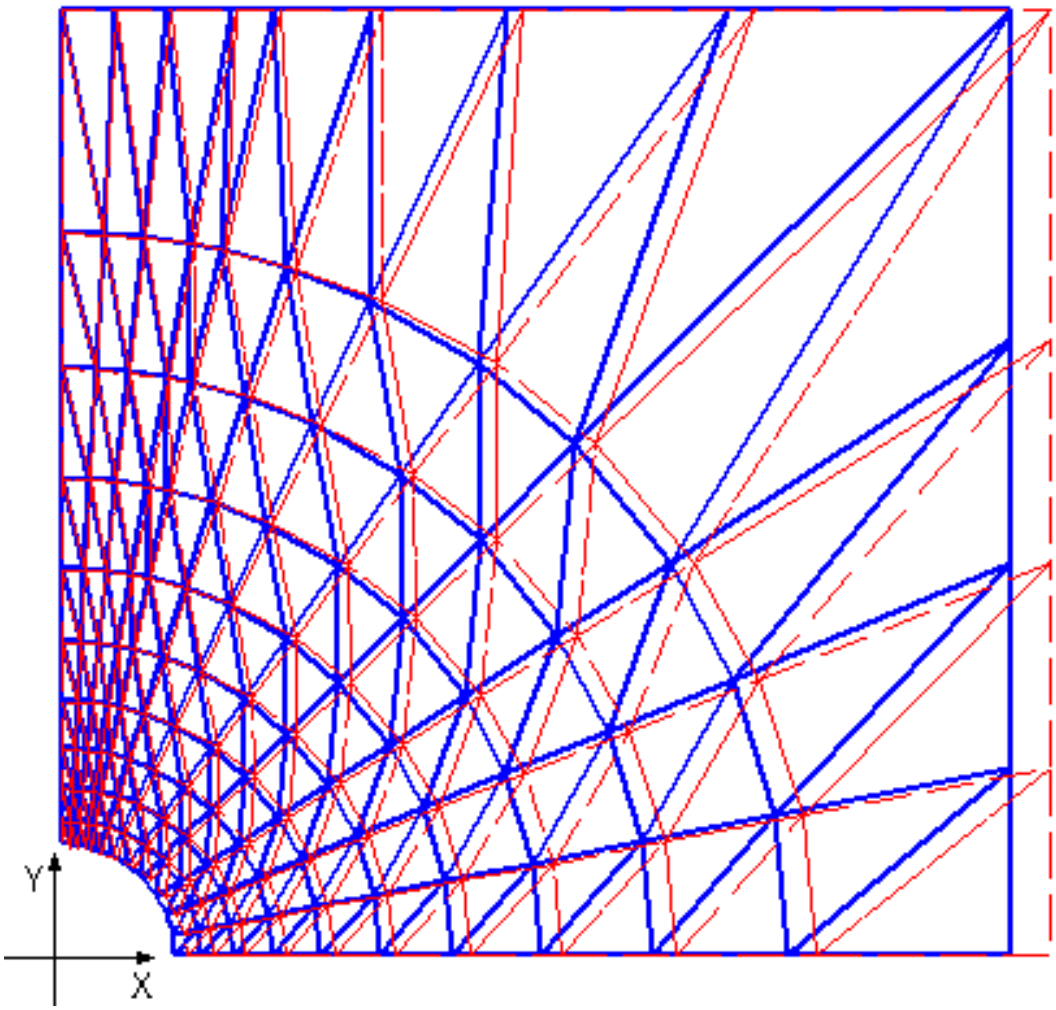

Figure 14. Nodal Displacement Diagram

1. Elastic Stress versus Strain Diagram

Since the applied strains can be modeled within the elastic region, it was simple to determine a stress strain state using this model. Figure 15 through Figure 17 are stress strain plot that compares the present solution to the published experimental results of Reference [20]. The three figures represent analysis performed on the laminated flat plate with a hole drilled through its center shown in Figure 13. The presented stress strain plots show good agreement with the analytical stress strain plots.

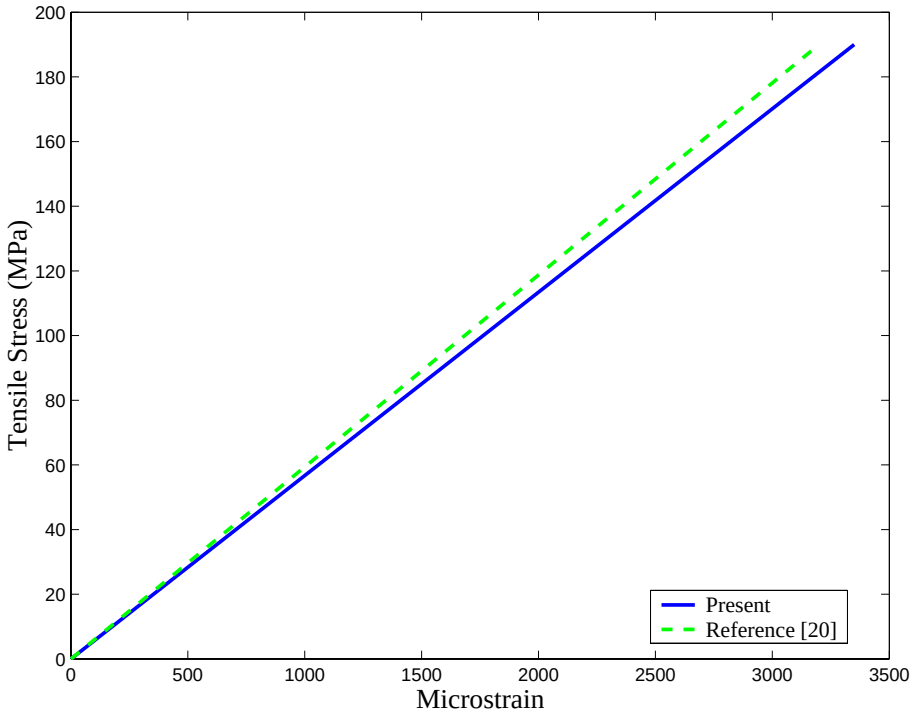

Figure 15. Stress-Strain Curve for a Flat Plate with a 3mm Circular Hole

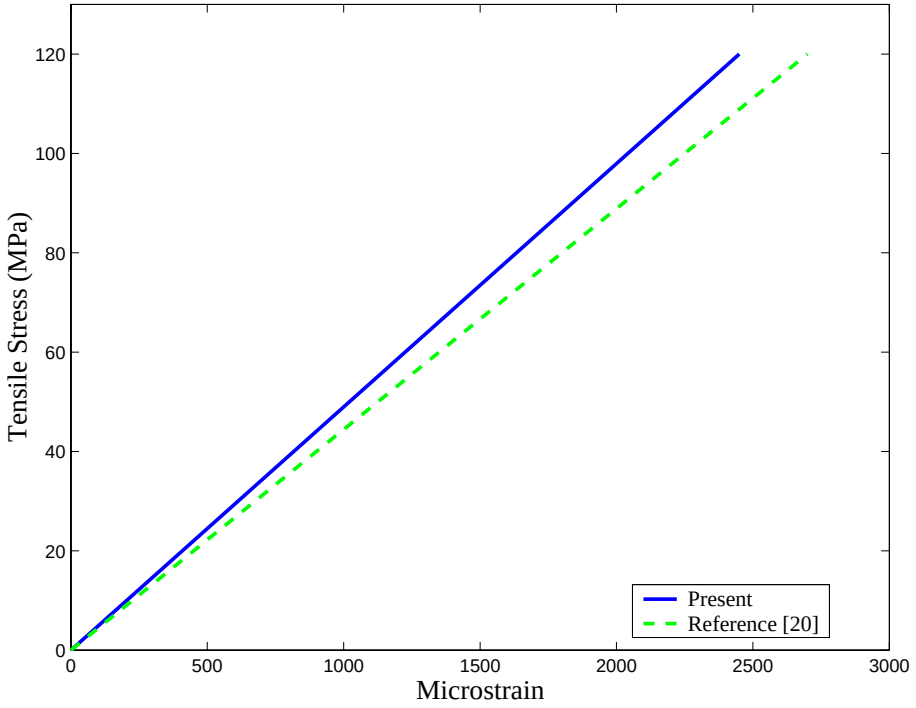

Figure 16. Stress-Strain Curve for a Flat Plate with a 6mm Circular Hole

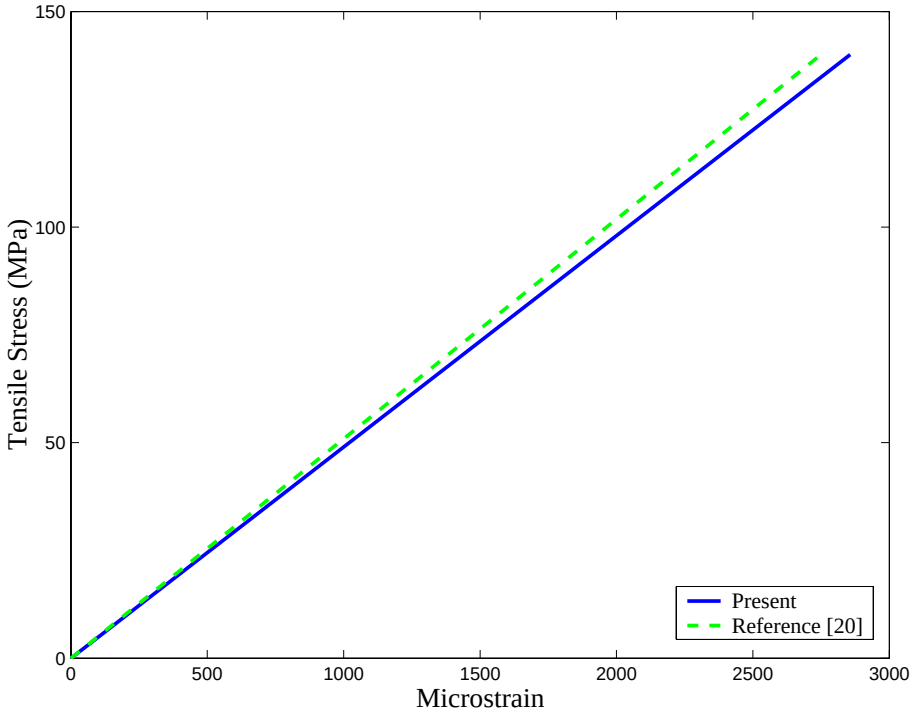

Figure 17. Stress-Strain Curve for a Flat Plate with a 9mm Circular Hole

2. Failure Analysis

The iso-strain condition was incrementally increased until the failure criterion is realized in the element of interest. In this case, the elements of interest are those corresponding to the virtual strain gage in Figure 13a. This is the site that classical solid mechanics predicts for fracture initiation. Because of the high volume fraction of the fibers, the ultimate strength of the fibers was set as the failure criterion for this analysis. With every incremental increase in global strain, the Multi-Scale model was used to determine the stresses in the fibers. Whenever a fiber reaches its ultimate strength, the material property at the point is degraded in the finite element model. The results are tabulated in Table 5. The ultimate failure strengths of the three composite plates with circular holes were predicted using the present analysis model and compared to the experimental data obtained by Ng *et al*. [20]. The presented predicted strengths are close to both experimental and previously predicted results.

HoleDiameter (mm)	*Experimental Strength (MPa)*[20]	*Predicted Strength (MPa)*[20]	*Predicted Strength (MPa)*[present]
3	435	499	494
6	395	460	438
9	333	377	354

Table 5. Predicted and Experimental Strengths for Plates with Circular Holes

C. AVERAGE SUBCELL STRESSES FOR THE UNIT CELL MODEL

Since a gross assumption of the unit cell model is that the strains are constant in each sub-cell, it may be of interest to determine how the sub-cell stresses compare to the average strains in the sub-cells of the MSC PATRAN/NASTRAN® finite element model. The sub-cell stresses for the unit cell model were determined using Equation (20).

$$\varepsilon_{ii}^{wf} = \left[T\right]^{-1} \varepsilon_{i}^{n} \tag{20}$$

The following strains were applied to the woven fabric for the sake of analysis.

$$\varepsilon_{ii}^{wf} = \begin{Bmatrix} .016 \\ -.0009 \\ 0 \end{Bmatrix}$$

The finite element model was divided into *volumes* which corresponded to the sub-cells of the unit cell model. The finite element *volume* strains were determined in two ways. First the average of the strains for all elements contained in the finite element volume were calculated. As a second check an average nodal displacement on two opposing faces was calculated. The difference in the average nodal displacement for each face (L_f) was divided by the original face length (L_o) to determine an average strain in the volume, as shown in Equation (21). Figure 18 shows the un-deformed and deformed sub-cells. Only the strains in the direction of applied stress were compared, the y-direction for this case.

$$\overline{\varepsilon_2^n} = \frac{Lf - Lo}{Lo} \tag{21}$$

The strains for all unit-cell model sub-cells are tabulated in Table 6. For the sake of brevity, 3 sub-cells were chosen for comparison with the finite element model. Those comparisons are tabulated in Table 7. The sub-cell numbers correspond to the number in Figure 10.

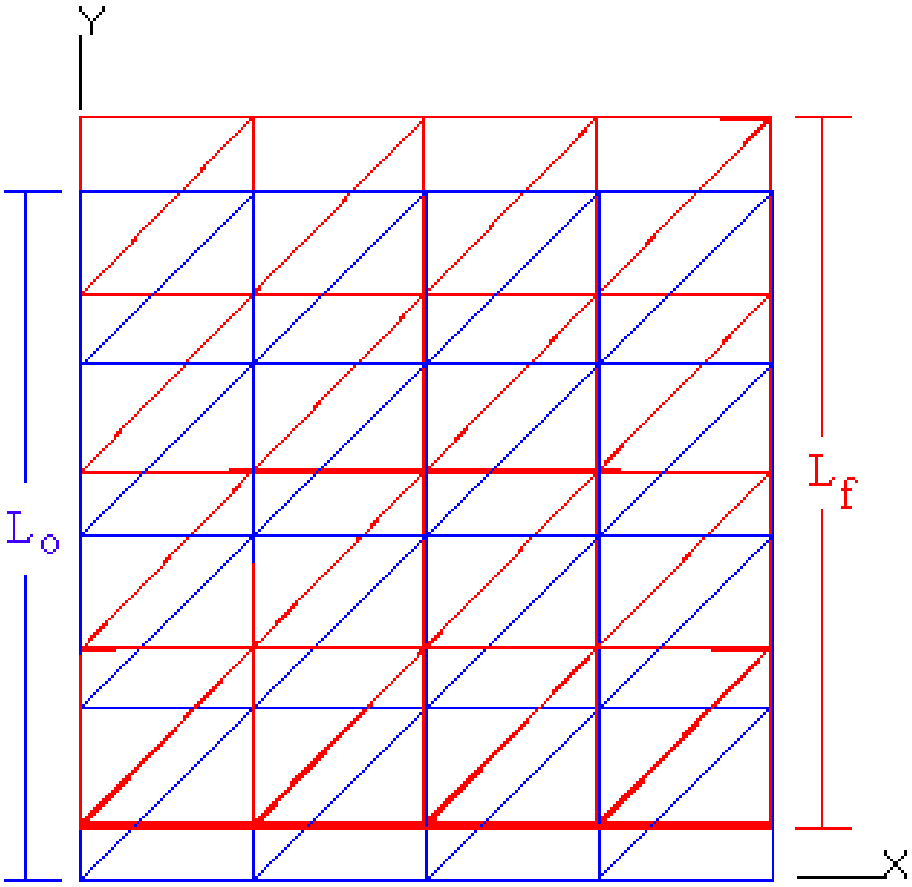

Figure 18. Deformed Finite Element Model

SUBCELL	X strain	Y strain	Z strain
1	0.001	0.0221	-0.0204
2	-0.0007	0.0139	-0.0102
3	-0.0007	0.0139	-0.0102
4	-0.003	0.0165	-0.0102
5	-0.003	0.0165	-0.0102
6	0.0054	0.0006	-0.0101
7	-0.0008	0.0162	-0.0103
8	-0.0008	0.0162	-0.0103
9	0.0054	0.0006	-0.0101
10	-0.0039	0.0303	-0.0158
11	-0.0057	0.0164	-0.0046
12	-0.0057	0.0164	-0.0046
13	-0.0039	0.0303	-0.0158
14	0.0014	0.0138	-0.0204
15	0.0014	0.0138	-0.0204
16	0.0009	0.021	-0.0204
17	0.0009	0.021	-0.0204

Table 6. Unit Cell Sub-cell Strains

SUBCELL	Unit Cell Model	Finite Element Model
1	0.0221	0.0277
4	0.0165	0.0142
11	0.0164	0.0150

Table 7. Comparison of Strains for Selected

THIS PAGE INTENTIONALLY LEFT BLANK

V. CONCLUSION

The multi-level and multi-scale model presented here provides a computationally efficient tool for analysis of a laminated composite structure made of 2/2-twill woven fabric composites. The analysis model was based on three independent modules: fiber-strand, strand-fabric, and lamination modules. Each module can communicates with its neighbor bi-directionally or be used independently. The major contribution of this work was the 2/2-twill composite unit cell and a finite element model to use for comparison. The unit cell consisted of only 77 sub-cells, while the finite element model consisted of 13456 finite elements.

The fiber-strand module of the multi-level model proved accurate in predicting effective composite strand material properties from those of the constituent fiber and matrix. Similarly, the strand-fabric module, utilizing the 2/2-twill unit cell, was assessed in predicting woven fabric material properties from composite strands properties. The results from the aforementioned modules were deemed accurate by comparison with published results for 3 separate 2/2-twill composites.

The unit cell model was also used to predict reduced transverse effective stiffness as a function of reduced matrix stiffness. This prediction compared favorable with published data from Ref. [18]. The 2/2-twill unit cell was further analyzed under an iso-strain condition to determine the average strains in the individual sub-cells. A finite element model, initially used to validate the assumptions of the unit cell model, was analyzed under the same iso-strain condition and used for comparison. It was found that the subcell strains of the unit cell model agreed well with the strains of the finite element model for the same volumes.

The multi-level and multi-scale analysis tool was used to conduct a detailed study of 3 plates. The plates were 2/2-twill composites laminates with the same dimensions, but 3 different sized center-drilled holes. The model was successful in:

1. Predicting stress versus strain plots for the plates. These plots produced effective moduli that agreed well with published results.

2. Describing progressive damage in the laminated plates at the basic material constituent levels, the fiber and matrix.

3. Predicting strength of each plate within 10% of the published experimental data for the same analysis.

VI. RECOMMENDATIONS

This work has shown that the multi-level multi-scale analysis utilizing a unit cell model is a viable alternative to a full finite element analysis for predicting stiffnesses and strengths, as well as progressive failures. This process lends itself to a plethora of other analyses and much additional work is required for more accurate predictions of the composite properties can be made. It is recommended that further study be conducted in the following areas:

1. The present study analyzed a flat laminated plate with a center-drilled hole subjected to an iso-strain condition. It is recommended that further studies be conducted using the 2/2-twill unit cell on other geometries. It is also recommended that other applied loads be considered.

2. Although not exploited in the present work, the 2/2-twill model has the ability to represent the more complex hybrid specimens. Further analysis is required to determine if the accuracy shown in the present work is maintained for hybrid composites.

3. It is recommended that unit cells be formulated for other woven fabrics such as satins, other twills, baskets, or leno weaves and used in the Multi-Level and Multi-Scale Analysis.

4. Parametric studies should be performed to determine the accuracy of the model for differing laminated geometries.

THIS PAGE INTENTIONALLY LEFT BLANK

LIST OF REFERENCES

[1] Ishikawa, T. and Chou, T. W., "One-Dimensional Micromechanical Analysis of Woven Fabric Composites", *AIAA Journal*, 1983, **21** (12), 1714-1721.

[2] Zhang, Y. C. and Harding, J., "A Numerical Micromechanics Analysis of the Mechanical Properties of a Plain Weave Composite", *Computers & Structures*, **36** (5), 1990, pp. 839-844.

[3] Naik, N. N. and Shembekar, P. S., "Elastic Behavior of Woven Fabric Composites: I-Lamina Analysis", *J. Composite Materials*, **26** (15), 1992, pp. 2196-2225.

[4] Naik, N. N. and Ganesh, V. K., "Prediction of on-axes Elastic Properties in of Plain Weave Fabric Composites", *Composite Science and Technology*, 1992, **26** (15) pp. 2196-2225.

[5] Cox, B.N., Carter, W.C. and Fleck, N.A., "A Binary Model of Textile Composite-I. Formulation." *Acta Materialia*, 1994, **42** (10), pp. 463-3479.

[6] Thompson D. M. and Criffin, "Crossply Laminates with holes in Compression: Straight Free Edge by 2-D to 3-D global/local Finite Element Analysis", *Journal of Composite Engineering*, 1993, **9**, pp. 745-756.

[7] Whitcomb, J. and Srirengan, K., "Effect of Various Approximations on Predicted Progressive Failure in Plain Weave Composites", *Composite Structures*, 1996, **34**, pp. 13-20.

[8] Scida, D., Aboura, Z., Benzeggagh, M., and Bocherens, E., "A Micromechanics Model for 3D Elasticity and Failure of Woven-Fibre Composite Materials", *Composite Science and technology*, 1999, **59**, pp. 505-517.

[9] Chaphalkar, P. and Kelkar, A., "Semi-Analytical Modeling of Progressive Damage in Twill Woven Textile Composites", *Recent Advances in Solids and Structures-2001,* IMECE2001, PVP-25212, 2001.

[10] Ng, S. Tse, P., and Lau, K., "Numerical and experimental determination of in-plane elastic Properties of 2/2-twill Weave Fabric Composites", *Composites. Part B: Engineering*, 1998, **29** (6), pp. 735-744.

[11] Kwon, Y. W., "Calculation of Effective Moduli of Fibrous Composites with or without Micro-mechanical Damage", *Composite Structures,* 1993, **25**, pp. 187-192.

[12] Kwon, Y. W. and Berner, J. M., "Micro-mechanics Model for Damage and Failure Analyses of Laminated Fibrous Composites", *Engineering Fracture Mechanics*, 1995, **52**, pp. 231-242.

[13] Kwon, Y. W. and Craugh, L. E., "Progressive Failure Modeling in Notched Cross-Ply Fibrous Composites", *Applied Composite Materials*, 2001, **8**, pp. 63-74.

[14] Kwon, Y. W. and Altekin, A., "Multi-level, Micro/Macro-Approach for Analysis of Woven Fabric Composite Plates", *Journal of Composite Materials*, Accepted for publication.

[15] Garnich, M. R. and Hansen, A. C., "A Multicontinuum Theory for Thermal-Elastic Finite Element Analysis of Composite Materials", *J. Composite Materials*, **31** (1), 1996, pp. 71-86.

[16] Pecknold, D. A. and Rahman, S., "Micromechanics-Based Structural Analysis of Thick Laminated Composites", *Computers and Structures*, **51** (2), 1994, pp. 163-179.

[17] Kwon, Y. W. and Bang, H.C., *The Finite Element Method Using Matlab*, 2nd ed., CRC Press, Boca Raton, Florida, 2000.

[18] Chaphalkar, P. and Kelkar, A., "Analytical and Experimental Elastic Behavior of Twill Woven Laminate", *Proceedings of the 12th International Conference on Composite Materials,* Paris, France, July 1999.

[19] Scida, D., Aboura, Z., Benzeggagh, M., and Bocherens, E., "Prediction of the Elastic Behaviour of Hybrid and Non-Hybrid Woven Composites", *Composite Science and technology*, 1997, **57,** pp. 1727-1740.

[20] Ng, S. Tse, P., and Lau, K., "Progressive Failure Analysis of 2/2-Twill Weave Fabric Composites with Moulded-in Circular Hole *Composites. Part B: Engineering*, 1998, **32** (2), pp. 139-152.

INITIAL DISTRIBUTION LIST

1. Defense Technical Information Center
   Ft. Belvoir, VA

2. Dudley Knox Library
   Naval Postgraduate School
   Monterey, CA

3. Professor Young W. Kwon
   Department of Mechanical Engineering
   Naval Postgraduate School
   Monterey, CA

4. Department Chairman
   Department of Mechanical Engineering
   Naval Postgraduate School
   Monterey, CA

5. Engineering and Technology Curriculum Code 34
   Monterey, CA

6. Lt. Kevin K. Roach
   Marietta, GA

THIS PAGE INTENTIONALLY LEFT BLANK